Chao *et al. Cancer Nanotechnology* (2025) 16:7
https://doi.org/10.1186/s12645-024-00304-z

Cancer Nanotechnology

RESEARCH Open Access

A novel photocleavable amino-modified graphene for covalent purification of N-glycans from hepatocellular carcinoma patients' serum for potential biomarkers discovery

Xuyuan Chao[1], Shengjie Yang[1,3], Baoying Zhang[1], Xin Zang[1], Jingyi Zhang[1], Xizi Liu[2], Lu Chen[1], Lu Qi[1], Xiaofeng Xue[2], Han Hu[2*] and Xinghe Wang[1*]

*Correspondence: huhan@caas.cn; wangxh@bjsjth.cn

[1] Phase I Clinical Trial Center, Beijing Shijitan Hospital, Capital Medical University, Beijing 100038, People's Republic of China
[2] Institute of Apicultural Research, Chinese Academy of Agricultural Sciences, No. 1 Beigou Xiangshan, Beijing 100093, People's Republic of China
[3] Phase I Clinical Trial Center, Shandong Cancer Hospital and Institute, Shandong First Medical University and Shandong Academy of Medical Sciences, Jinan 250117, People's Republic of China

Abstract

Glycosylation alterations have emerged as significant indicators in the landscape of cancer diagnosis, with aberrant N-glycans standing out as potential biomarkers. The existing methods for purifying N-glycans mainly rely on their hydrophilicity, affinity, and size. These methods exhibit relatively weak binding forces and low specificity based on non-covalent interactions. Moreover, the current liquid chromatography-based N-glycan purification and detection techniques must be bettered for clinical settings' rapid diagnostic requirements. Here, we have developed a method involving the covalent binding of graphene modified with photocleavable amino groups to N-glycans in hepatocellular carcinoma (HCC) patients' serum glycoproteins. The N-glycans are identified using MALDI-TOF/TOF MS, catering to the requirements of biological research and the diagnosis of liver cancer disease. Specifically, amino-functionalized graphene is linked with photocleavable groups bearing hydrazide functional group, then undergoes acyl hydrazone covalent reaction with aldehyde groups on the side chains of oxidized monosaccharides to capture the N-glycans. Finally, under UV irradiation at a wavelength of 356 nm for 15 s, the ortho-nitrobenzyl photocleavable groups undergo cleavage, completing the release of captured N-glycans, which are then subjected to MALDI-TOF/TOF MS mass spectrometry for detection. Our findings demonstrate significant differences in the N-glycan profiles between serum samples of liver cancer patients and healthy individuals. These differences are characterized by increased abundance and molecular weight of N-glycans. Through biomarker screening, one N-glycan with an m/z ratio of 1847.01 shows the potential to serve as a diagnostic biomarker for liver cancer ($P < 0.05$). Our research underscores the potential of photocleavable amino-modified graphene for detecting aberrant N-glycans in HCC patients' serum to elucidate the intricate between aberrant N-glycan alterations and HCC. This research paves the way for developing novel biomarkers, diagnostic strategies, and therapeutic interventions to combat this complex disease.

Keywords: Photocleavable amino graphene, N-Glycans, Human serum, Hepatocellular carcinoma, Cancer biomarker, MALDI-TOF/TOF MS

Graphical Abstract

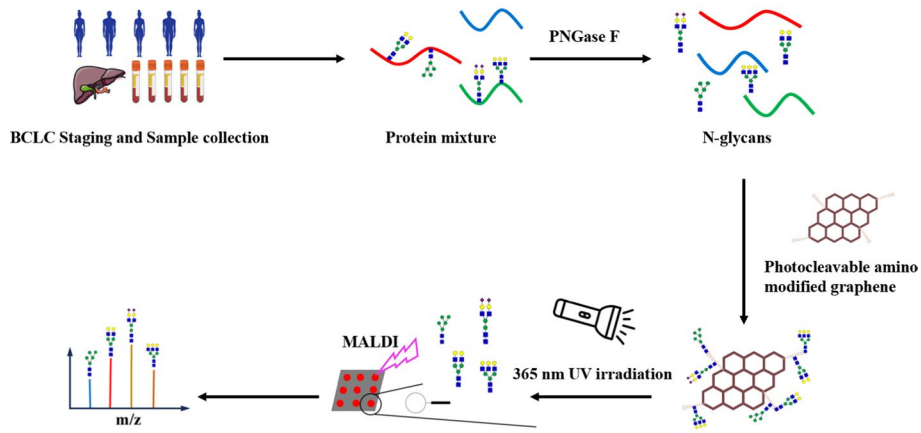

Introduction

Hepatocellular carcinoma (HCC) is the sixth most common cancer and the third leading cause of cancer-related mortality worldwide (Llovet et al. 2021). Patients with early-stage HCC typically benefit from curative treatments, achieving a 5-year survival rate exceeding 70%. However, due to insufficient early detection methods, only 20–30% of individuals diagnosed with HCC qualify for curative interventions, such as surgical resection, liver transplantation, or ablative techniques(Bruix and Sherman 2005, 2011; Parikh et al. 2020).

Blood is conveniently collected in clinical settings, and diagnostic biomarkers in blood are the most feasible for diagnosing cancer. For example, alpha-fetoprotein (AFP) is primarily used to monitor treatment response and recurrence in HCC patients (Crandall 1981). Carcinoembryonic antigen (CEA) is used primarily to diagnose and monitor colorectal cancer. Still, elevated levels can also be detected in other types of cancer, such as breast, lung, and pancreatic cancers (Hall et al. 2019). Prostate-specific antigen (PSA) is used for early prostate cancer screening, diagnosis, and treatment monitoring (Adhyam and Gupta 2012).

Glycosylation, a common post-translational modification, involves the attachment of sugars to proteins or lipids, leading to significant structural and functional alterations in eukaryotic cell proteins. N-glycosylation, the predominant form of protein glycosylation, is substantial in modifying proteins, including those found in human blood (Ramazi and Zahiri 2021). Previous studies have highlighted how specific modifications in protein glycosylation, particularly those involving N-glycan structures, may hold promise as potential serum biomarkers for early cancer detection. These modifications can influence various biological processes, such as cell–cell interactions, immune response, and tumor progression, making them valuable indicators of malignancy. For instance, alterations in N-glycan branching and fucosylation patterns have been associated with several types of cancer, including HCC (Nie et al. 2015), ovarian cancer (Chen et al. 2017), and breast cancer (Lee et al. 2020). Consequently, developing analytical methods to characterize and quantify these glycan changes in

patient serum could significantly enhance early diagnostic capabilities and improve clinical outcomes through timely intervention.

Human serum is a complex sample, and purifying N-glycans from it is not easy. Non-glycosylated proteins, nucleic acids, and electrolytes in serum can interfere with the purification and detection of target N-glycans. Existing methods for purifying or enriching N-glycans on glycoproteins are primarily based on properties such as hydrophilicity, affinity, and size (Riley et al. 2021). However, these methods, which rely on non-covalent interactions, have weak binding forces and low specificity. Moreover, due to the inherent heterogeneity of glycans, nonspecific binding is common, necessitating multiple steps like incubation, washing, and elution with functionalized fillers, which are cumbersome and prone to sample loss (Alla and Stine 2022). Compared to non-covalent methods, covalent-based purification or enrichment methods offer advantages like more robust selectivity, high efficiency, and minimal sample loss (Zhu et al. 2017). While covalent-based methods are widely used in the purification or enrichment of N-glycopeptides, they have yet to be applied in the purification or enrichment of N-glycans (Bai et al. 2018).

Graphene is a single layer of carbon atoms arranged in a two-dimensional honeycomb lattice. It is the basic building block of other carbon-based materials such as graphite, carbon nanotubes, and fullerenes. Graphene has an exceptionally large surface area and flexible structure, suitable for purifying or enriching glycans in complex biological samples (Klukova et al. 2016). Although graphene has yet to be widely applied in the purification and separation of N-glycans, graphite, similar to graphene, is extensively used in this area (Riley et al. 2021). Traditionally, the purification and separation of N-glycans by graphite mainly involve non-covalent interactions. Graphite retains N-glycans through hydrophilic interactions or inducing dipole–dipole interactions on its surface with charged N-glycans (West et al. 2010; Sheng et al. 2021). Qian XH et al. utilized commercial graphite carbon black columns to enrich N-glycans from glycoproteins and subjected them to derivatization treatment. They successfully identified 26 and 9 glycoforms in ovalbumin from chicken egg whites and fetal bovine serum, respectively (Tong et al. 2012). Beyond merely using the adsorption properties of carbon materials, researchers developed different types of porous carbon materials, leveraging their size effects to separate N-glycans and proteins effectively. For example, Zou HF et al. synthesized porous carbon materials with a specific surface area of 1576.0 m^2/g and a pore size of 3.4 nm using sucrose as the carbon source. They successfully used these materials to enrich N-glycans from the serum of liver cancer patients, identifying 32 N-glycans. Compared to the serum results from normal individuals, the abundance of 5 glycoforms was significantly increased, and 4 of these glycoforms were core-fucosylated (Qin et al. 2011).

Photolabile linker groups, due to their advantages of readily available light sources and good controllability, are widely used in fields such as solid-phase synthesis, protease activity assays, and substance delivery (Bochet 2002). Ortho-nitrobenzyl linker groups are the earliest developed and most commonly used photolabile linkers. Compared to other groups, they exhibit high photolysis rates and stability with relatively mild reaction conditions. Under UV light exposure, they undergo proton transfer and efficiently cleave within 0.17 min.

We have combined ortho-nitrobenzyl linker groups with graphene, where the terminal groups contain amino functionalities that can react with the aldehyde groups on N-glycan side chains. Through the formation of a covalent hydrazone bond, N-glycans are captured. Brief UV irradiation releases the captured N-glycans, which are then analyzed using MALDI-TOF/TOF MS. The entire process takes approximately 6 h and 30 min, and with pre-treated human serum N-glycans prepared in advance, the duration can be shortened to approximately 2 h, significantly reducing the time compared to other liquid chromatography–mass spectrometry (LC–MS) based detection methods and making it suitable for rapid clinical testing. After specifically purifying serum N-glycans from healthy volunteers and HCC patients, irradiation with 365 nm UV light for 10–20 s released them. The purified glycans were identified using MALDI-TOF/TOF MS. The analysis revealed that an m/z ratio of 1847.01 could serve as a potential biomarker for liver cancer ($P < 0.05$), establishing a new method for purifying and identifying N-glycans in complex biological systems.

Results

Development of novel photocleavable amino-modified graphene for infrared characterization

We synthesized photocleavable amino-modified graphene. The schematic diagram of the synthesized photocleavable amino-modified graphene is shown in Fig. 1. The amino groups of graphene can covalently bind to the reducing end aldehyde of N-glycans, achieving particular enrichment of glycans. On the other hand, ortho-nitrobenzyl linkage groups, the photocleavable linkage, can undergo proton transfer under UV light irradiation, resulting in cleavage within 0.17 min and the release of bound N-glycans for mass spectrometry detection.

Figure 2 shows the infrared spectra of the raw material (a) and the synthesized product (b). In the raw material's spectrum, peaks at 1665.98 cm^{-1}, 1571.40 cm^{-1}, and 1212.39 cm^{-1} indicate the presence of carbonyl and aromatic structures. In contrast, the product's spectrum features new peaks at 3325.28 cm^{-1} (O–H stretching), 1539.65 cm^{-1} (N–O stretching), and other characteristic peaks, suggesting the introduction of hydroxyl and nitro groups. The disappearance of the carbonyl peak and the appearance of these new peaks confirm that a chemical transformation has occurred, altering the molecular structure of the raw material.

Table 1 presents the infrared spectroscopy characterization results of the characterization of the raw material reduced graphene oxide and the synthesized product photocleavable amino-modified graphene.

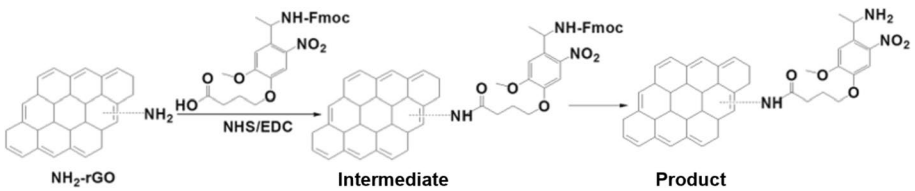

Fig. 1 Synthesis of photocleavable amino-modified graphene

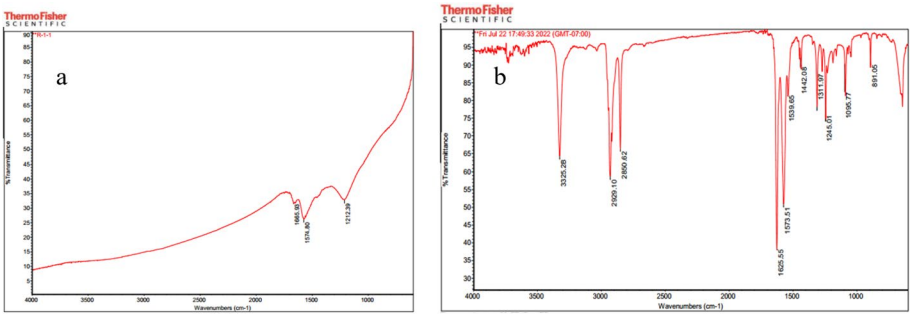

Fig. 2 The infrared spectra of the raw material (**a**) and the synthesized product (**b**)

Table 1 The infrared spectroscopy characterization results of the characterization of the raw material reduced graphene oxide and the synthesized product photocleavable amino-modified graphene

Infrared attribution of product	**cm^{-1}**	**Functional group**
1	3325	v_{NH}
2	2929	$v_{C\text{-}H}$
3	2850	$v_{\text{-}CH2\text{-}}$
4	1625	$ß_{NH}$ or δ_{NH}
5	1573	$v_{C=C}$
6	1539	v_{NO2}
7	1442	v_{NO2}
8	1311	v_{NO2}
9	1245	$v_{C\text{-}N}$
10	1095	$v_{C\text{-}O\text{-}C}$
11	891	$Yv_{C=C}$
Infrared attribution of raw materials	cm^{-1}	
1	1574	$v_{C=C}$
2	1212	$ß_{C\text{-}H}$
Infrared attribution of raw materials	**cm^{-1}**	
1	1574	$v_{C=C}$
2	1212	$ß_{C\text{-}H}$

We used maloheptaose as the standard sugar chain, captured with photocleavable amino-modified graphene, and obtained MALDI-TOF/TOF MS spectra, as shown in Fig. 3. The obtained [M + Na] + peak was observed at 1173.2353 m/z with a 4983 intensity value, demonstrating that photocleavable amino-modified graphene can capture sugar chains and accomplish photolytic cleavage release. The molecular weight of maloheptaose is 1153 Da. After capture with photocleavable amino-modified graphene and subsequent photolytic cleavage, entering MALDI-TOF/TOF MS, the end oxygen atoms of the sugar chain were replaced by nitrogen atoms, resulting in a decrease in molecular weight of 2 Da. In MALDI-TOF/TOF MS, glycans are typically detected as sodium adducts $[M + Na]^+$ as molecular ions, with the relative atomic mass of sodium being 23 Da. For maltoheptaose, which has a molecular weight of 1153 Da, oxidation by sodium periodate removes 2 hydrogen atoms, resulting in a molecular weight of 1151 Da. When this oxidized maltoheptaose (1151 Da)

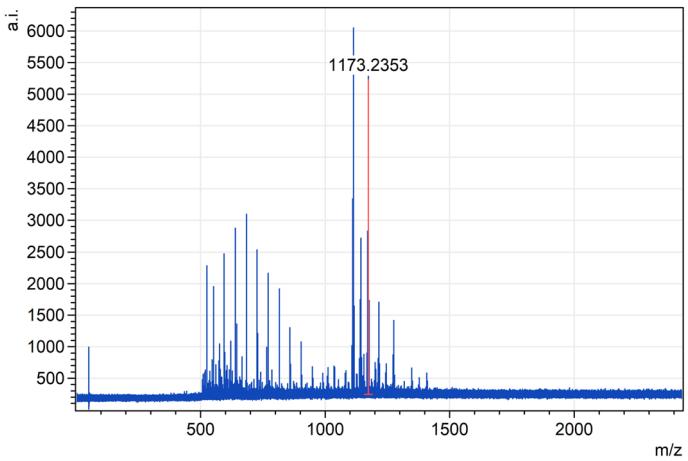

Fig. 3 Photocleavable amino-modified graphene-captured maltoheptaose MALDI-TOF/TOF MS spectra

binds to photocleavable amino-modified graphene and is subsequently released, it gains 1 hydrogen atom (1 Da) while an oxygen atom (16 Da) is replaced by a nitrogen atom (14 Da), leading to a net loss of 2 Da. Including the sodium ion (23 Da), the mass

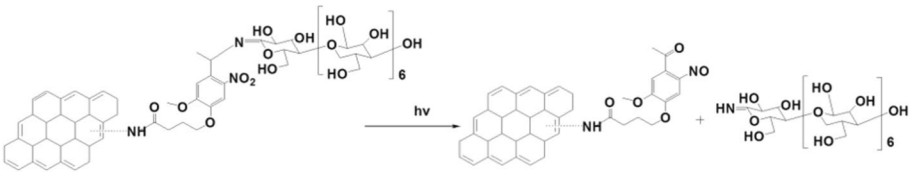

Fig. 4 The capture of oxidized maltoheptaose using photocleavable amino-modified graphene and photolytic release

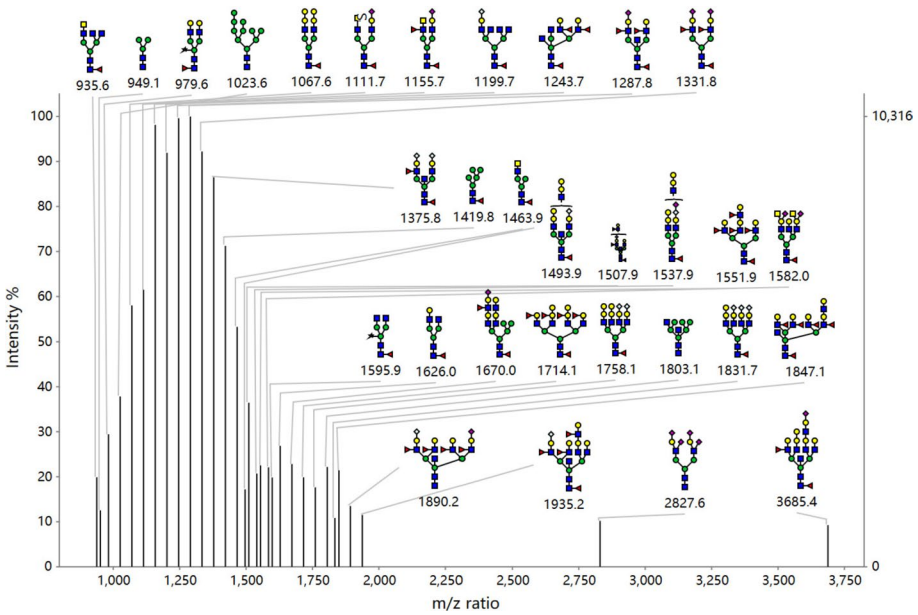

Fig. 5 MALDI-TOF/TOF spectrum of N-glycans purified from human serum using photocleavable amino-modified graphene

spectrum shows a peak at 1173 Da. The schematic diagram is shown in Fig. 4. One of the MALDI-TOF/TOF spectra of N-glycans purified from human serum using photocleavable amino-modified graphene is shown in Fig. 5. The corresponding ^{1}H NMR spectroscopy is shown in Fig S1. A single peak at δ 5.76 (s, 1H) indicates a hydrogen atom near a double bond, showing that the terminal oxygen atoms of the sugar chain have been replaced by nitrogen atoms.

HCC patients exhibit significant differences in serum N-glycan compared to healthy individuals

In our experiment, photocleavable amino-modified graphene captured 6085 and 2913 N-glycans from 20 μL serum samples obtained from 15 HCC patients and eight healthy individuals, respectively. HCC patients have an average of 406 N-glycans per sample, while healthy individuals have an average of 354 N-glycans per sample. We observed significant differences ($p < 0.05$) in the N-glycan profiles between serum samples from HCC patients and healthy individuals, with an increased number and m/z ratio of N-glycans in the serum of HCC patients.

The box plot in Fig. 6a illustrates the distribution of N-glycan m/z ratios across various glycan structures labeled from G2 to Z14. Each box plot represents the data's interquartile range (IQR) for a specific glycan, with the line inside each box indicating the median m/z ratio. Whiskers extend to the smallest and largest values within 1.5 times the IQR from the lower and upper quartiles, respectively, while outliers are shown as individual points. Green represents the healthy volunteer group, while other colors represent the different Barcelona Clinic Liver Cancer (BCLC) stages of the liver cancer patients group. Compared to the healthy volunteers group, the HCC patients group has more outliers in the serum N-glycan m/z ratios. Figure 6b presents a Venn diagram that compares N-glycans' presence in healthy and cancer samples. The blue circle represents N-glycans found exclusively in healthy samples (754 glycans), while the red circle represents those unique to cancer samples (2110 glycans). The overlap in purple indicates N-glycans common to both health conditions, amounting to 431 glycans. This diagram effectively highlights the substantial difference in glycosylation

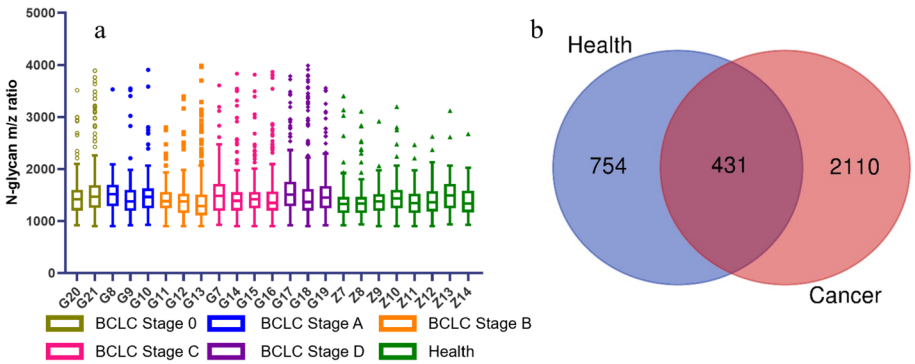

Fig. 6 **a**. The box plot compares the m/z ratio of N-glycans in the serum of HCC patients and healthy individuals. **b** The Venn diagram compares N-glycan profiles in serum samples from HCC patients and healthy individuals after removing duplicate values

patterns between healthy and cancerous states, suggesting specific glycans that could be potential biomarkers for cancer diagnosis or therapeutic targets.

The serum N-glycan profiles differ among HCC patients of different BCLC stages

The Barcelona Clinic Liver Cancer (BCLC) staging system is a clinical staging system for HCC (Reig et al. 2022). It categorizes HCC patients into several stages, each with distinct treatment strategies and prognoses. BCLC staging is assessed based on tumor characteristics, liver function, and overall patient status. For both doctors and patients, understanding the BCLC stage of the patient can aid in selecting the most appropriate treatment approach and evaluating the patient's prognosis. We divided each serum sample into two groups, with three replicates per group, resulting in 138 spectra and 8998 N-glycan m/z ratios. Subsequently, principal component analysis (PCA) was conducted without setting a specific number of components, with a variance covered value of 0.95. Figure 7 illustrates the PCA plot of N-glycans in serum. The 3D scatter plot illustrates the distribution of N-glycan profiles across healthy volunteers and HCC patients at various stages according to the BCLC staging system. Each colored cube represents a different group: green for healthy individuals, cyan for BCLC Stage 0, blue for Stage A, purple for Stage B, yellow for Stage C, and orange for Stage D. The axes (PC1, PC2, and PC3) represent the first three principal components derived from principal component analysis (PCA), summarizing the most significant variance in the dataset. The clustering of green cubes indicates that healthy individuals have similar N-glycan profiles, while the distinct spread of other colors shows that cancer patients exhibit varying profiles as

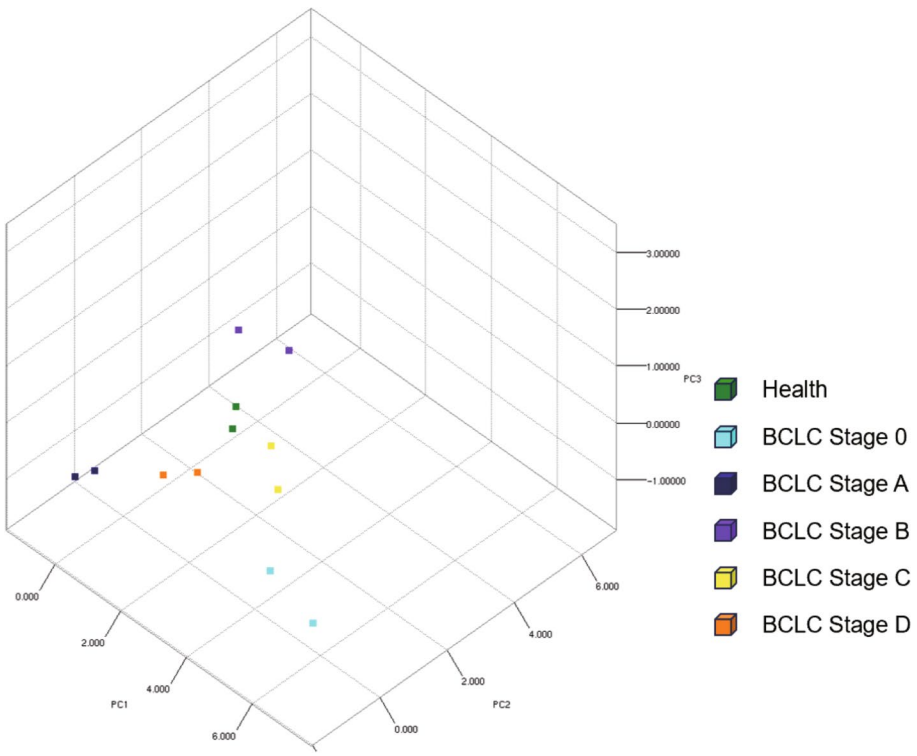

Fig. 7 PCA plot of N-glycans purified by photocleavable amino-modified graphene from human serum

the disease progresses. This separation highlights the potential of N-glycan profiles as biomarkers for distinguishing between healthy states and different stages of HCC. After removing duplicates, Venn diagrams were used to classify N-glycans in patients' blood at different stages (Fig. 8). The Venn diagram illustrates the distribution of unique and shared N-glycans in the serum of patients at different BCLC stages. Each colored area in the diagram represents a specific BCLC stage (blue for Stage 0, red for Stage A, green for Stage B, yellow for Stage C, and brown for Stage D). The numbers indicate the count of distinct N-glycans detected at each stage, as well as their overlap across multiple stages. For stage-specific N-glycans, 298 unique N-glycans were found only in Stage 0. In Stage A, 296 unique N-glycans were identified. Stage B showed 414 unique N-glycans, Stage C had 336 unique N-glycans, and Stage D exhibited 471 unique N-glycans. Regarding overlaps between stages, for instance, 136 N-glycans were shared between Stage 0 and Stage D, but were absent in the other stages (A, B, and C). Stage A and Stage B shared 163 N-glycans. In some cases, multiple stages shared certain N-glycans, such as 27 N-glycans being common to Stages 0, A, C, and D. For the sections where the intersection is 0, there are no shared N-glycans between certain stages. For example, the intersection between Stages 0, A, and C shows 0, indicating that these stages do not share any N-glycans. This suggests that HCC patients at different BCLC stages produce different types of N-glycans, with some overlap in the types of glycans. Figure 6 displays the numbers of different N-glycans in patients' blood at different BCLC stages. A summary of the principal component analysis and detailed lists of Venn diagrams are provided in the Supplementary Data.

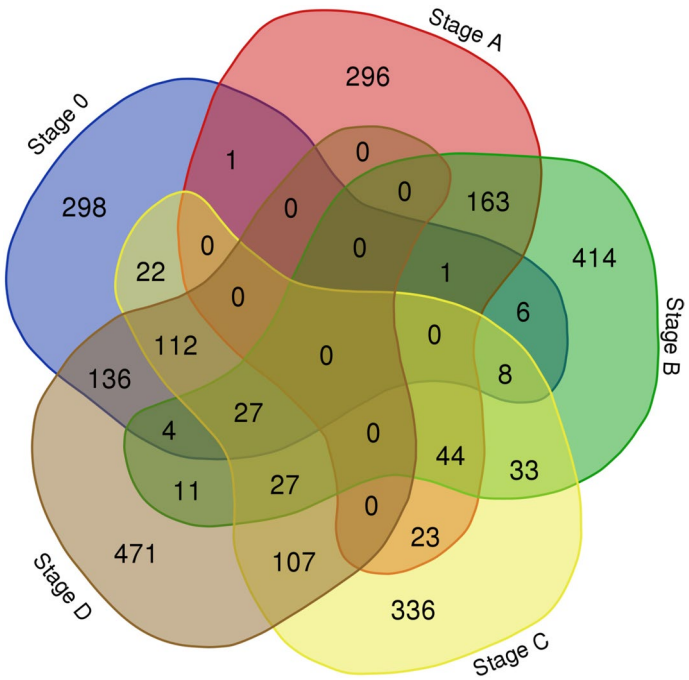

Fig. 8 The numbers of different N-glycans in patients' blood at different BCLC stages

Using photocleavable amino-modified graphene to purify N-glycans from human serum can reveal potential biomarkers for HCC

We grouped N-glycan m/z ratios by BCLC stages, performed randomization tests, and used the machine learning algorithm to build a well-performing classification model. There are 58 numbers of m/z ratios with p-values < 1. Only in the blood of HCC patients are 63 N-glycan m/z ratios. There are three numbers of m/z ratios with p-values < 0.05, namely 980.5226 ($p < 0.02$), 1713.9786 ($p < 0.02$), and 1847.0115 ($p < 0.03$), among which m/z 980.5226 appears in BCLC Stage C and healthy individuals grouping, m/z 1713.9786 appears in BCLC Stage A and Stage C, as well as healthy individuals grouping. m/z 1847.0115 is observed in BCLC Stage 0 and D. The potential structure of m/z 1847.0115 was identified in the Glycome DB database as a bisected fucosylated N-glycan, suggesting that this N-glycan with m/z 1847.0115 might be a potential biomarker for HCC. The inferred structure of m/z 1847.0115 N-glycan is shown in Fig. 9. Detailed lists of all biomarkers are provided in the supplementary data.

The novel photocleavable amino-modified graphene method identified more diverse glycans in human serum than the strong anion exchange and electrostatic repulsion hydrophilic interaction chromatography (SAX-ERLIC) method

The strong anion exchange and electrostatic repulsion hydrophilic interaction chromatography (SAX-ERLIC) method is a chromatography technique used to selectively enrich glycopeptides by combining strong anion exchange with electrostatic repulsion and hydrophilic interaction, allowing for effective separation of glycopeptides

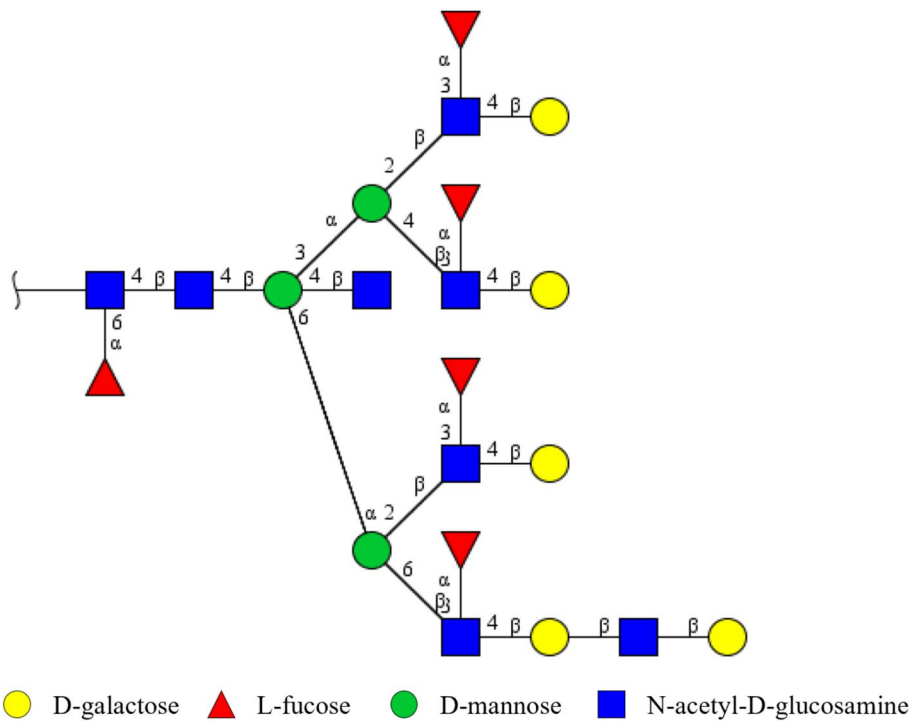

Fig. 9 The inferred structure of m/z 1847.0115 N-glycan, $[M + Na + H]^+$

from complex biological samples (Chao et al. 2024). We applied the SAX-ERLIC strategy to purify glycopeptides from serum, followed by LC–MS identification. The identified glycopeptides were analyzed using Byonic software and matched against the *Homo sapiens* glycoprotein database downloaded from UniProt to provide detailed information on serum glycans.

Fig. S2 shows a Venn diagram comparing glycans detected by the SAX-ERLIC method and those detected by the novel photocleavable amino-modified graphene method in human serum. After removing duplicates, the SAX-ERLIC method, represented by the purple circle, identified 126 unique glycans, while the novel photocleavable amino-modified graphene method, shown in the orange circle, detected 723 unique glycans. The overlapping region contains 37 glycans identified by both methods, indicating some overlap but also a substantial number of unique glycans detected by each approach. Compared to the SAX-ERLIC method, the novel photocleavable amino-modified graphene method detected a greater number of glycans across the human serum sample, revealing notable differences in the types of glycans identified by each approach. The detailed data are provided in the supplementary materials.

Materials and methods

Design and synthesis of photocleavable amino-modified graphene

Graphene can be chemically modified to introduce specific functional groups, forming new chemical bonds and undergoing complex functionalization processes, which exhibit stability and ease of handling. Dissolve 500 mg of 4-[4-(1-(Fmoc-amino)ethyl)-2-methoxy-5-nitrophenoxy]butanoic acid (Thomas Scientific) in 20 mL DMF (Sigma-Aldrich). Then, sequentially add 100 mg of reduced graphene oxide (Sigma-Aldrich), 5 g of EDCI (Sigma-Aldrich), and 5 g of HOBt (Sigma-Aldrich) into the reaction system. Under vigorous stirring, react at room temperature for 7 days to synthesize the intermediate. Filter the intermediate after synthesis, wash the filter cake with DMF and dichloromethane (Sigma-Aldrich), dry the obtained solid, and directly conduct the deprotection reaction without further treatment. Dissolve 258 mg of intermediate in 10 mL DMF, then add 10 mL of pyridine. Under vigorous stirring, react at room temperature for one day. After completion of the reaction, filter, wash the filter cake with DMF and dichloromethane, and dry the obtained solid to obtain photocleavable amino-modified graphene.

Staging of HCC patients and grouping of serum samples

We collected serum samples from 15 patients clinically diagnosed with HCC and 8 serum samples from healthy volunteers. The serum samples from HCC patients were categorized into stages 0 to D according to the Barcelona Clinic Liver Cancer (BCLC) staging, forming five groups. Detailed information about sex, age, and the BCLC staging group is shown in Table S1 in the Supplementary data.

Isolating N-glycans from human serum

The serum is stored in a −80 °C ultra-low temperature freezer; thaw slowly in a 4 °C refrigerator before use, and gently mix the serum after thawing. Ultrafiltration of

20 μL serum through a 30-kDa ultrafiltration tube, mixing the filtered serum with an equal volume containing 1 mM DTT (Sigma-Aldrich) and 200 mM NH_4HCO_3 (Sigma-Aldrich). The mixture was shaken at 65 ˚C, 1500 rpm for 5 min to achieve moderate denaturation. Addition of 400U PNGase F enzyme (New England Biolabs), followed by incubation at 37 ˚C, 500 rpm for 30 min. After brief centrifugation, 400 μL cold ethanol (Fisher Chemical) was added for precipitation at −80 °C for 1 h. Centrifugation at 12,000 × g for 2 min to collect the supernatant containing N-linked glycans, transfer to another tube, and lyophilize.

Purification of N-glycans using photocleavable amino-modified graphene

Before combining with photocleavable amino-modified graphene, N-glycans need to be oxidized. Oxidize N-glycans following the method developed by Zhang et al. (Zhang et al. 2003). The dried N-glycans are oxidized at room temperature in 100 mM sodium acetate (Sigma-Aldrich) and 150 mM NaCl (Sigma-Aldrich) (pH 5.5) with a final concentration of 15 mM sodium periodate (Sigma-Aldrich) in the dark shaking for 1 h. Then, 20 mmol/L of freshly prepared sodium sulfite is added to the reaction mixture, followed by shaking for 10 min. After consuming excess oxidant, the solution is lyophilized.

1.5 mg of photocleavable amino-modified graphene was washed with methanol (Fisher Chemical) three times to remove impurities. The oxidized N-glycans are reacted with photocleavable amino-modified graphene in a solution of 95% methanol (containing 0.5% acetic acid) at 90 °C with shaking for 30 min. Additional reaction solutions can be added as needed during the process. After the reaction, wash non-specifically adsorbed materials five times with the reaction solution and centrifuge to remove the supernatant. Add 200 μL of the reaction solution, irradiate under a 365 nm UV light source for 15 s, and centrifuge at 1200 g for 10 min. The supernatant contains purified N-glycans transferred to a new tube for heat drying. The same treatment was used for 10 mM aqueous maltoheptaose solution. The water used in all experiments was purified using a Milli-Q Plus system (Millipore). The schematic diagram is shown in Fig. 4.

MALDI-TOF/TOF MS data acquisition

Bruker UltrafleX III MALDI-TOF/TOF mass spectrometer (Bruker, Daltonics, Germany) was used for glycan detection. Data acquisition was performed in positive reflector mode with an acceleration voltage of 20 kV, a scan range of m/z 1000–4000, and laser energy of 6000. The final spectra were obtained by accumulating 1000 laser shots for spectrum averaging. The matrix consisted of a 50% acetonitrile and 50% 0.1% trifluoroacetic acid solution containing 10 mg/mL of 2,5-dihydroxybenzoic acid. 1 μL of the sample to be analyzed was air-dried on a stainless-steel plate, followed by adding 1 μL of the matrix to allow for complete crystallization before analysis. One of the MALDI-TOF/TOF spectra of N-glycans purified from human serum using photocleavable amino-modified graphene is shown in Fig. 9.

Data analysis

Upload the peak list generated by MALDI-TOF/TOF MS to the software GlycoWorkbench developed by Haslam et al. for determining the glycan structures

(Ceroni et al. 2008) and match the experimental mass peaks with the glycan m/z values recorded in the GlycomeDB database (Ranzinger et al. 2011). Normality and lognormality tests were used to check for normality, and the Kolmogorov–Smirnov test was used to assess significance. The statistical analyses were conducted using GraphPad Prism software, version 8.0 for Windows (GraphPad Software, La Jolla, California, USA). Principal component analysis, discovery of biomarkers, and cross-validation experiments were performed using Mass-up software (López-Fernández et al. 2015). In Mass-up software, We grouped the 8998 N-glycan m/z ratios purified from human serum using photocleavable amino-modified graphene according to BCLC stages. We performed independent randomization tests based on 10,000 replications and Benjamini–Hochberg FDR for intra-strain and inter-strain calculations, obtaining p-values and q-values for candidate biomarkers. Using the lazy-IBk algorithm based on Weka to train instances in the data to construct a model for cross-validation experiment, the results show that the model has good classification performance (kappa value 0.7).

Sample preparation of serum glycans using SAX-ERLIC strategy followed by LC – MS analysis

Add 20 μL of serum to four times the volume of cold acetone, then precipitate at −20 °C for 2 h. Centrifuge at 8000 × g at 4 °C for 15 min, discard the supernatant and air-dry the serum proteins for 15 min. Resuspend the proteins in 100 μL of 5 M urea and determine the protein concentration using a Bradford Protein Assay kit (Beyotime Biotechnology). Take a 200 μg protein sample, reduce it with 10 mM dithiothreitol for 1 h, and alkylate with 50 mM iodoacetamide in the dark for another hour. Digest the protein sample with sequencing-grade trypsin (Promega) for 12 h at an enzyme-to-protein ratio of 1:50 (w/w) and terminate the digestion by adding 1 μL formic acid (Sigma-Aldrich).

Glycopeptides were collected using SOLA SAX SPE Cartridge (Thermo Fisher Scientific, CAT No. 60109–003), following the protocol described by Bermudez and Pitteri(Bermudez and Pitteri 2021). Briefly, reconstitute the sample in 50% acetonitrile (ACN) (Sigma-Aldrich) and 0.1% trifluoroacetic acid (TFA) (Sigma-Aldrich), and prepare the cartridge by wetting with ACN and conditioning with 100 mM Triethylammonium acetate (pH 7.0) (Sigma-Aldrich). Wash the cartridge with water, equilibrate with 95% ACN, and 1.0% TFA, then add the 60 μL sample, allowing it to flow through slowly. Wash again with 95% ACN and 1.0% TFA, and finally elute the bound glycopeptides using 50% ACN and 0.1% TFA.

Samples were reconstituted in 0.1% TFA (5 μL injected) and separated using a 120-min gradient on a Thermo Vanquish Neo UHPLC coupled to an Orbitrap Ascend Tribrid mass spectrometer. A fused silica C18 column (50 μm ID, 350 mm) (Agilent Technologies) was used with mobile phase A as 0.1% formic acid and mobile phase B as 80% acetonitrile with 0.1% formic acid. MS1 scans (300–1800 m/z) were acquired at 120 K resolution, and MS2 scans with EThcD fragmentation at 60 K resolution. Data analysis was performed using Byonic software against the *Homo sapiens* glycoprotein database downloaded from UniProt.

Discussion

HCC is accompanied by changes in glycosylation, typically involving alterations such as increased fucosylation of core and outer-arm structures, elevated expression of high-mannose structures, heightened levels of fucosylated, sialylated, and complex N-glycans, and an increase in α-1,3-fucosylated branching on triantennary glycans, among other changes, which result in a higher m/z ratio due to an increased amount of monosaccharides attached to the outer part of these N-glycans (de Oliveira et al. 2018).

Research on the N-glycan profile in human serum can provide new avenues for developing diagnostic and therapeutic strategies for HCC (de Oliveira et al. 2018). However, human blood's components such as proteins, nucleic acids, electrolytes, etc., can interfere with analyzing and detecting relatively low-abundance N-glycan chains. Therefore, developing a material that can rapidly purify serum N-glycan chains is crucial.

Graphene possesses an extremely large specific surface area (approximately 2630 m^2/g) and a flexible structure (Azam et al. 2017), theoretically capable of increasing the loading capacity of N-glycan chains and reducing steric hindrance with enriched N-glycan chains, thus enhancing the scale and efficiency of enrichment. Existing methods for enriching N-glycan chains based on carbon materials are achieved through non-covalent means. However, the principles by which carbon materials retain glycan chains (dipole, hydrophilicity, charge induction, dispersion, etc.) are not very clear (Riley et al. 2021). Moreover, collecting adsorbed N-glycans or glycopeptides depends on solvent conditions during non-covalent enrichment or purifying methods [26]. After surface modification, graphene can form covalent or non-covalent interactions with glycosidic bonds, specifically enriching N-glycans or N-glycopeptides. Researchers have introduced various enrichment moieties, endowing graphene with good affinity and selectivity, enabling efficient enrichment of N-glycans or N-glycopeptides from complex biological samples. In previous studies, Bi et al. developed hydrophilic chitosan-functionalized magnetic graphene nanocomposites, enriching 393 N-linked glycopeptides from a 200 μg human renal mesangial cell tryptic digest (Bi et al. 2020). Kong et al. designed a boronic acid (BA)-functionalized mesoporous graphene–silica composite for isolating intact glycopeptides from complex biological samples, identifying 724 N-linked glycopeptides from 20 μL of human serum (Kong et al. 2021). Bai et al. used hydrazide-functionalized hydrophilic polymer hybrid graphene oxide, identifying 480 N-glycopeptides from 10 μL of human serum (Bai et al. 2017). It should be noted that our study focused on N-glycomics and did not include research on peptide glycosylation, while the information on N-glycan glycosylation sites also contains valuable information in HCC glycoproteomics. Ignoring this aspect would limit the depth of exploration into protein glycosylation associated with HCC.

Some precedents exist for using MALDI-TOF/TOF MS in human serum glycomics research to screen for HCC-related biomarkers. Goldman et al. used MALDI-TOF MS to identify three HCC-related N-glycans from human serum. Tang et al. discovered seven N-glycans related to cancer in the serum of HCC patients using MALDI-TOF MS data. Kamiyama et al. identified N-glycans with m/z ratio values of 2890.052 and 3560.295 from human serum as biomarkers for diagnosing HCC using MALDI-TOF and TOF/TOF MS. The research on human serum N-glycomics is of significant value for the diagnosis or treatment of HCC. We did not conduct quantitative research on

the purification of human serum N-glycans using photocleavable amino-modified graphene because the N-glycans purified by photocleavable amino-modified graphene are oxidized non-reducing sugars, and there is currently no suitable MS2-based isotope labeling method for non-reducing polysaccharide.

We applied oxidized graphene material for the first time to covalently enrich N-glycan chains, developing novel photocleavable amino-modified graphene utilizing the principle of hydrazide chemistry covalent enrichment (Zhang et al. 2003). Initially, the cis-dihydroxyl groups on the side chains of the glycan were oxidized to aldehydes, which then reacted covalently with amino groups on the new material to form hydrazone bonds, thereby capturing the glycans. Innovatively, we combined the adjacent nitro-benzyl connecting group as a photocleavable group with graphene material, allowing captured glycan chains to be cleaved off by UV irradiation at 365 nm for 15 s and detected by MALDI-TOF/TOF MS without further derivatization. With pre-treated samples, this method delivers strong signals, requires approximately 2 h, and is well-suited for the rapid clinical detection of serum N-glycans in HCC patients. Compared to LC–MS, N-glycan chains purified by photocleavable amino-modified graphene do not require further derivatization to obtain better signals. N-glycan chains released by UV irradiation at 365 nm from the photocleavable amino-modified graphene covalently bound to them contain NH groups. NH groups may increase the ionization efficiency of N-glycan chains, as amino groups can form ion pairs with protons, thereby aiding in generating more ionized products. This increase in ionization efficiency may positively impact the overall ionization efficiency, contributing to enhancing N-glycan mass spectrometry signal intensity and analysis sensitivity.

The potential tumor biomarker we identified, an m/z 1847.0115 N-glycan, belongs to the bisected fucosylated N-glycans class of glycans that may play a pivotal role in hepatocellular carcinoma (HCC) development and progression. These glycans align with emerging data suggesting that bisected fucosylated N-glycans may contribute to several HCC-associated mechanisms, including enhanced cell adhesion, immune modulation, and tumor progression (Lin and Lubman 2023). The structural variations in N-glycans, particularly fucosylation, play a crucial role in HCC progression by modulating cell adhesion and immune evasion. Fucosylation, which adds fucose residues to N-glycan structures, alters cell-surface interactions and promotes tumor cell adhesion, which is critical for metastasis. In HCC, increased core fucosylation is linked to the enhanced binding of surface proteins, such as epidermal growth factor receptor (EGFR), to their ligands, which stimulates cell proliferation and migration (Wang and Chen 2023a). These changes can also affect adhesion molecules, such as E-cadherin, which is essential for maintaining cell–cell adhesion and tissue integrity, thus facilitating tumor cell detachment and metastatic spread (Pinho et al. 2010). These findings highlight the importance of bisected fucosylated N-glycans in modifying the adhesion capabilities of HCC cells and ultimately contributing to disease aggressiveness. In addition to promoting cell adhesion, bisected fucosylated N-glycans have immunomodulatory functions within the tumor microenvironment, a property that is particularly relevant in HCC. Elevated levels of fucosylated glycoproteins in the serum of HCC patients are associated with immunosuppressive effects, potentially reducing the immune response to the tumor. These glycoproteins may suppress T cell activity or modify macrophage

function, thus fostering a microenvironment that favors tumor survival and growth (Yi et al. 2015). By evading immune detection, HCC cells with increased bisected fucosylated glycans can thrive within the immunosuppressive niche, highlighting these glycans as potential tumor markers and modulators of immune evasion (Wang and Chen 2023b). Enzyme-driven alterations in glycan structure further contribute to HCC's invasive and migratory characteristics of HCC. In HCC, enzymes such as GnT-IVa, which enhance the production of complex bisected fucosylated N-glycans, are upregulated, promoting cell motility and invasiveness (Nie et al. 2015). High levels of bisected fucosylated N-glycans support not only structural, but also functional changes, enhancing the ability of tumor cells to interact with the extracellular matrix and invade surrounding tissues (Mereiter et al. 2019). The bisected fucosylated N-glycans may indicate poor prognosis in HCC patients, underscoring the importance of these glycans as biomarkers and potential therapeutic targets for monitoring HCC progression (Thomas et al. 2020).

This study represents preliminary exploration. Future research endeavors should prioritize identifying appropriate quantitative methods for N-glycomics compatible with photocleavable amino-modified graphene. Furthermore, it will be essential to compare this novel material with commonly used substances for purifying N-glycan chains from complex biological samples, typically employing the hydrazone method. Although this study screened potential HCC biomarkers from a comprehensive set of 8998 N-glycans, we recognize that the sample size of 15 HCC patients and 8 healthy individuals is a limitation for broader biomarker discovery. Expanding the serum sample cohort to include more patients across diverse HCC subtypes and clinical stages is essential to further strengthen the generalizability and stability of the identified potential biomarkers.

Conclusions

In conclusion, our study presents a pioneering method employing photocleavable amino-modified graphene for the covalent enrichment of N-glycan chains from human serum, addressing the need for rapid and efficient biomarker discovery in HCC patients. This innovative approach bypasses the limitations of conventional non-covalent methods, offering enhanced specificity and efficiency. Our findings reveal significant differences in N-glycan profiles between HCC patients and healthy individuals, highlighting N-glycans' potential as diagnostic biomarkers for HCC. Notably, one N-glycan with an m/z ratio of 1847.01 emerges as a promising candidate for further clinical validation. Moreover, the entire process is convenient and rapid, aligning with the demands of clinical diagnostics. By leveraging the unique properties of graphene and photocleavable amino groups, our study sheds light on the intricate interplay between aberrant N-glycan alterations and HCC progression, paving the way for developing novel diagnostic strategies and therapeutic interventions in combating this complex disease.

Abbreviations

HCC	Hepatocellular carcinoma
MALDI-TOF/TOF MS	Matrix-assisted laser desorption/ionization time-of-flight/time-of-flight mass spectrometry
AFP	Alpha-fetoprotein
CEA	Carcinoembryonic antigen
PSA	Prostate-specific antigen
LC–MS	Liquid chromatography–mass spectrometry
BCLC	The Barcelona clinic liver cancer

PCA	Principal component analysis
DMF	N, N-Dimethylformamide
EDCI	1-Ethyl-3-(3-dimethylaminopropyl)carbodiimide
HOBt	Hydroxybenzotriazole
DTT	Dithiothreitol
SAX-ERLIC	Strong anion exchange and electrostatic repulsion hydrophilic interaction chromatography
ACN	Acetonitrile
TFA	Trifluoroacetic acid

Supplementary Information

The online version contains supplementary material available at https://doi.org/10.1186/s12645-024-00304-z.

Additional file 1: Fig S1. Photocleavable amino-modified graphene-captured maltoheptaose ^{1}H NMR spectroscopy.

Additional file 2: Fig S2. Comparison of glycan profiles identified by SAX-ERLIC and photocleavable amino-modified graphene methods in human serum.

Additional file 3.

Additional file 4.

Additional file 5.

Additional file 6: Table S1. The donor groups with BCLC staging.

Acknowledgements
Not applicable.

Author contributions
XYC, SJY, and BYZ contributed equally to this work. XYC, SJY, and BYZ: Sample Preparation, Investigation, Validation, Visualization, Analysis, Writing—Original Draft; XZ, JYZ, XZL, and LC: Visualization; LQ: Project Administration; HH: Supervision, Writing—Review & Editing, Resources; XFX: Resources; XHW: Conceptualization, Methodology, Supervision, Funding Acquisition, Resources. All authors reviewed the manuscript.

Funding
This work was supported by the National Natural Science Foundation of China (52073180).

Availability of data and materials
Data is provided within the manuscript or supplementary information files.

Declarations

Ethics approval and consent to participate
All human serum samples obtained have been approved by the Capital Medical University Affiliated Beijing Shijitan Hospital ethics committee (sjtky11-1x-2022-(052)) and adhere to the principles of the Helsinki Declaration.

Consent for publication
All authors have reviewed the manuscript and consent to this publication.

Competing interests
The authors declare no competing interests.

Received: 2 June 2024 Accepted: 26 December 2024
Published online: 17 February 2025

References

Adhyam M, Gupta AK (2012) A review on the clinical utility of PSA in Cancer Prostate. Indian J Surg Oncol 3:120–129. https://doi.org/10.1007/s13193-012-0142-6

Alla AJ, Stine KJ (2022) Recent strategies for using monolithic materials in glycoprotein and glycopeptide analysis. Separations 9:44. https://doi.org/10.3390/separations9020044

Azam MA, Zulkapli NN, Dorah N, Seman RNAR, Ani MH, Sirat MS, Ismail E, Fauzi FB, Mohamed MA, Majlis BY (2017) Review—critical considerations of high quality graphene synthesized by plasma-enhanced chemical vapor deposition for electronic and energy storage devices. ECS J Solid State Sci Technol 6:M3035–M3048. https://doi.org/10.1149/2.0031706jss

Bai H, Pan Y, Guo C, Zhao X, Shen B, Wang X, Liu Z, Cheng Y, Qin W, Qian X (2017) Synthesis of hydrazide-functionalized hydrophilic polymer hybrid graphene oxide for highly efficient *N*-glycopeptide enrichment and identification by mass spectrometry. Talanta 171:124–131. https://doi.org/10.1016/j.talanta.2017.04.076

Bai H, Pan Y, Qi L, Liu L, Zhao X, Dong H, Cheng X, Qin W, Wang X (2018) Development a hydrazide-functionalized thermosensitive polymer based homogeneous system for highly efficient N-glycoprotein/glycopeptide enrichment from human plasma exosome. Talanta 186:513–520. https://doi.org/10.1016/j.talanta.2018.04.098

Bermudez A, Pitteri SJ (2021) Enrichment of intact glycopeptides using strong anion exchange and electrostatic repulsion hydrophilic interaction chromatography. Methods Mol Biol 2271:107–120. https://doi.org/10.1007/978-1-0716-1241-5_8
Bi C, Yuan Y, Tu Y, Wu J, Liang Y, Li Y, He X, Chen L, Zhang Y (2020) Facile synthesis of hydrophilic magnetic graphene nanocomposites via dopamine self-polymerization and Michael addition for selective enrichment of N-linked glycopeptides. Sci Rep 10:71. https://doi.org/10.1038/s41598-019-56944-4
Bochet CG (2002) Photolabile protecting groups and linkers. J Chem Soc Perkin Trans 1:125–142. https://doi.org/10.1039/B009522M
Bruix J, Sherman M (2005) Management of hepatocellular carcinoma. Hepatology 42:1208–1236. https://doi.org/10.1002/hep.20933
Bruix J, Sherman M (2011) Management of hepatocellular carcinoma: an update. Hepatology 53:1020–1022. https://doi.org/10.1002/hep.24199
Ceroni A, Maass K, Geyer H, Geyer R, Dell A, Haslam SM (2008) GlycoWorkbench: a tool for the computer-assisted annotation of mass spectra of glycans. J Proteome Res 7:1650–1659. https://doi.org/10.1021/pr7008252
Chao X, Zhang B, Yang S, Liu X, Zhang J, Zang X, Chen L, Qi L, Wang X, Hu H (2024) Enrichment methods of N-linked glycopeptides from human serum or plasma: a mini-review. Carbohyd Res 538:109094. https://doi.org/10.1016/j.carres.2024.109094
Chen H, Deng Z, Huang C, Wu H, Zhao X, Li Y (2017) Mass spectrometric profiling reveals association of N-glycan patterns with epithelial ovarian cancer progression. Tumour Biol 39:101042831771624. https://doi.org/10.1177/1010428317716249
Crandall BF (1981) Alpha-fetoprotein: a review. Crit Rev Clin Lab Sci 15:127–185. https://doi.org/10.3109/10408368109105870
de Oliveira RM, Ornelas Ricart CA, Araujo Martins AM (2018) Use of mass spectrometry to screen glycan early markers in hepatocellular carcinoma. Front Oncol. https://doi.org/10.3389/fonc.2017.00328
Hall C, Clarke L, Pal A, Buchwald P, Eglinton T, Wakeman C, Frizelle F (2019) A review of the role of carcinoembryonic antigen in clinical practice. Annal Coloproctol 35:294. https://doi.org/10.3393/ac.2019.11.13
Klukova L, Filip J, Belicky S, Vikartovska A, Tkac J (2016) Graphene oxide-based electrochemical label-free detection of glycoproteins down to aM level using a lectin biosensor. Analyst 141:4278–4282. https://doi.org/10.1039/C6AN00793G
Kong S, Zhang Q, Yang L, Huang Y, Liu M, Yan G, Zhao H, Wu M, Zhang X, Yang P, Cao W (2021) Effective enrichment strategy using boronic acid-functionalized mesoporous graphene-silica composites for intact N- and O-linked glycopeptide analysis in human serum. Anal Chem 93:6682–6691. https://doi.org/10.1021/acs.analchem.0c05482
Lee SB, Bose S, Ahn SH, Son BH, Ko BS, Kim HJ, Chung IY, Kim J, Lee W, Ko M-S, Lee K, Chang S, Park HS, Lee JW, Kim D-C (2020) Breast cancer diagnosis by analysis of serum N-glycans using MALDI-TOF mass spectroscopy. PLoS ONE 15:e0231004. https://doi.org/10.1371/journal.pone.0231004
Lin Y, Lubman DM (2023) The role of N-glycosylation in cancer. Acta Pharmaceutica Sinica B 14:1098. https://doi.org/10.1016/j.apsb.2023.10.014
Llovet JM, Kelley RK, Villanueva A, Singal AG, Pikarsky E, Roayaie S, Lencioni R, Koike K, Zucman-Rossi J, Finn RS (2021) Hepatocellular carcinoma. Nat Rev Dis Primers 7:1–28. https://doi.org/10.1038/s41572-020-00240-3
López-Fernández H, Santos HM, Capelo JL, Fdez-Riverola F, Glez-Peña D, Reboiro-Jato M (2015) Mass-Up: an all-in-one open software application for MALDI-TOF mass spectrometry knowledge discovery. BMC Bioinformatics 16:318. https://doi.org/10.1186/s12859-015-0752-4
Mereiter S, Balmaña M, Campos D, Gomes J, Reis CA (2019) Glycosylation in the era of cancer-targeted therapy: where are we heading? Cancer Cell 36:6–16. https://doi.org/10.1016/j.ccell.2019.06.006
Nie H, Liu X, Zhang Y, Li T, Zhan C, Huo W, He A, Yao Y, Jin Y, Qu Y, Sun X-L, Li Y (2015) Specific N-glycans of hepatocellular carcinoma cell surface and the abnormal increase of Core-α-1, 6-fucosylated triantennary glycan via N-acetylglucosaminyltransferases-IVa regulation. Sci Rep 5:16007. https://doi.org/10.1038/srep16007
Parikh ND, Mehta AS, Singal AG, Block T, Marrero JA, Lok AS (2020) Biomarkers for the early detection of hepatocellular carcinoma. Cancer Epidemiol Biomark Prev 29:2495–2503. https://doi.org/10.1158/1055-9965.EPI-20-0005
Pinho SS, Seruca R, Gärtner F, Yamaguchi Y, Gu J, Taniguchi N, Reis CA (2010) Modulation of E-cadherin function and dysfunction by N-glycosylation. Cell Mol Life Sci CMLS 68:1011. https://doi.org/10.1007/s00018-010-0595-0
Qin H, Zhao L, Li R, Wu R, Zou H (2011) Size-selective enrichment of n-linked glycans using highly ordered mesoporous carbon material and detection by MALDI-TOF MS. Anal Chem 83:7721–7728. https://doi.org/10.1021/ac201198q
Ramazi S, Zahiri J (2021) Post-translational modifications in proteins: resources, tools and prediction methods. Database. https://doi.org/10.1093/database/baab012
Ranzinger R, Herget S, von der Lieth C-W, Frank M (2011) GlycomeDB-a unified database for carbohydrate structures. Nucleic Acids Res 39:D373-376. https://doi.org/10.1093/nar/gkq1014
Reig M, Forner A, Rimola J, Ferrer-Fábrega J, Burrel M, Garcia-Criado Á, Kelley RK, Galle PR, Mazzaferro V, Salem R, Sangro B, Singal AG, Vogel A, Fuster J, Ayuso C, Bruix J (2022) BCLC strategy for prognosis prediction and treatment recommendation: the 2022 update. J Hepatol 76:681–693. https://doi.org/10.1016/j.jhep.2021.11.018
Riley NM, Bertozzi CR, Pitteri SJ (2021) A pragmatic guide to enrichment strategies for mass spectrometry-based glycoproteomics. Mol Cell Proteomics 20:100029. https://doi.org/10.1074/mcp.R120.002277
Sheng Q, Li J, Chen Y, Liang X, Lan M (2021) Hydrophilic graphene oxide-dopamine-cationic cellulose composites and their applications in N-Glycopeptides enrichment. Talanta 226:122112. https://doi.org/10.1016/j.talanta.2021.122112
Thomas D, Rathinavel AK, Radhakrishnan P (2020) Altered glycosylation in cancer: a promising target for biomarkers and therapeutics. Biochim Biophys Acta 1875:188464. https://doi.org/10.1016/j.bbcan.2020.188464
Tong W, Han H, Song Z, Ma C, Pan Y, Zhang Y, Qin W, Qian X (2012) Chemical derivatization with a polycyclic aromatic hydrocarbon for highly sensitive detection of N-linked glycans using MALDI-TOF MS. Anal Methods-Uk 4:3531–3535. https://doi.org/10.1039/C2AY25663K
Wang Y, Chen H (2023a) Protein glycosylation alterations in hepatocellular carcinoma: function and clinical implications. Oncogene 42:1970–1979. https://doi.org/10.1038/s41388-023-02702-w

West C, Elfakir C, Lafosse M (2010) Porous graphitic carbon: a versatile stationary phase for liquid chromatography. J Chromatogr A 1217:3201–3216. https://doi.org/10.1016/j.chroma.2009.09.052

Yi C-H, Weng H-L, Zhou F-G, Fang M, Ji J, Cheng C, Wang H, Liebe R, Dooley S, Gao C-F (2015) Elevated core-fucosylated IgG is a new marker for hepatitis B virus-related hepatocellular carcinoma. Oncoimmunology 4:e1011503. https://doi.org/10.1080/2162402X.2015.1011503

Zhang H, Li X, Martin DB, Aebersold R (2003) Identification and quantification of N-linked glycoproteins using hydrazide chemistry, stable isotope labeling and mass spectrometry. Nat Biotechnol 21:660–666. https://doi.org/10.1038/nbt827

Zhu R, Zacharias L, Wooding KM, Peng W, Mechref Y (2017) CHAPTER 7: Glycoprotein enrichment analytical techniques: advantages and disadvantages. Methods Enzymol 585:397–429. https://doi.org/10.1016/bs.mie.2016.11.009

Publisher's Note